

Research Article

Open Access

Destruction of Polycrystalline Silver Sulphide Electrodes in a High Voltage Nanosecond Discharge at Atmospheric Pressure

OK Shuaibov*, OY Minya, RV Hrytsak, AI Pogodin, OM Malinin, AO Malinina, Yu Yu Bilak, RM Golomb and ZT Homoki

Department of Therapy, Head of the Council of Young Scientists, Uzhhorod National University, Ukraine

ABSTRACT

The results of the study of the characteristics and parameters of the plasma of a high-voltage nanosecond atmospheric pressure discharge between the electrodes of the superionic conductor - silver sulfide (Ag₂S) in argon are given. The discharge was ignited in argon at pressures of 13.3 - 101 kPa, the distance between the electrodes made of the polycrystalline Ag₂S compound was 2 mm. Destruction of the material of the electrodes during the discharge and introduction of silver sulfide vapors into the interelectrode space occurred due to microexplosions of natural inhomogeneities on the working surfaces of the electrodes. The discharge can be used as a point ultraviolet lamp on silver atoms and ions, which emits light in the spectral range of 200 - 330 nm or as a plasma chemical reactor for the synthesis of thin films based on silver sulfide.

*Corresponding author

OK Shuaibov, Department of Therapy, Head of the Council of Young Scientists, Uzhhorod National University, Ukraine.

Received: June 13, 2023; Accepted: June 21, 2023; Published: July 30, 2023

Keywords: Nanosecond Discharge, Argon, Silver Sulfide, Plasma

Introduction

The results of systematic studies of the characteristics of an overvoltage nanosecond discharge between electrodes made of copper, stainless steel, aluminum, and chalcopyrite (CuInSe₂) in air, nitrogen, and argon are given in [1]. Such a discharge can be a point source of ultraviolet radiation, and from its plasma it is possible to deposit thin nanostructured films of oxides of transition metals and chalcopyrite [2]. The introduction of electrode material into the plasma in these experiments occurs in the process of microexplosions of natural inhomogeneities of the electrode surface in a strong electric field during the formation and decay of ectons [3]. Ecton decay refers to the extinction (disappearance) of plasma formation, which was formed on the surface of the electrode as a result of a micro-explosion of micro- or nano-scale inhomogeneity in a strong electric field. The reason for this is the evaporation of the corresponding tip and the cessation of introduction of the electrode material into the plasma.

The films were deposited on a solid dielectric substrate installed near the electrode system. If the plasma of such discharges intensively emits ultraviolet radiation, then assisting the synthesis of thin films with ultraviolet allows influencing the surface nanostructures, in particular, reducing their resistance [4].

For many promising applications of thin films in technology, the synthesis of thin films with superionic conductivity is important [5]. This is necessary for the creation of technologies for the production of capacitors and large-capacity batteries, which are widely used in technology. Therefore, the search and optimization of new physical methods for the synthesis of film micro-nanostructures

based on massive polycrystalline superionic conductors of the Ag₂S, Ag₂Se type are currently relevant.

Our previous experiments on the synthesis of thin films based on the Ag₂S compound in air at atmospheric pressure showed that, in addition to silver sulfide, the synthesized thin film also contains impurities: silver sulfite (Ag₂SO₃) and silver sulfate (Ag₂SO₄) [6]. Therefore, an inert gas was chosen as a buffer gas in these experiments - argon, which does not enter into chemical reactions with vapors of the Ag₂S compound or products of its destruction in a nanosecond discharge plasma.

Currently, the characteristics and parameters of the plasma of a high-voltage nanosecond discharge in atmospheric pressure argon between silver sulfide electrodes have not been studied, which prevents the use of such discharges for the development of ultraviolet lamps at the transitions of atoms and singly charged silver ions in the spectral range of 200-330 nm, as well as plasma chemical reactors on the synthesis of thin films with superionic conductivity.

The article presents the results of the study of the characteristics and parameters of the plasma of a high-voltage nanosecond discharge between polycrystalline silver sulfide electrodes in atmospheric pressure argon.

Conditions and Techniques of the Experiment

An overvoltage nanosecond discharge was ignited in argon at pressures in the range of 13-101 kPa between electrodes made of the polycrystalline compound Ag₂S, which is a superionic conductor. This type of discharge is characterized by a sequence of voltage and current pulses lasting tens of nanoseconds. This

sequence is formed due to the mismatch of the output resistance of the high-voltage modulator and the plasma resistance and is the most optimal for the evaporation of inhomogeneities of the electrode surface by the ectonic mechanism and the synthesis of the corresponding films. The main factor for such an evaporation mechanism is the high impulse power of the discharge, which is characteristic only for discharges of nanosecond duration. The block diagram of the experimental setup and the structure of the discharge chamber is given in [1,6].

The ignition of the overvoltage nanosecond discharge took place with the help of a high-voltage modulator of bipolar voltage pulses with a total duration of 50-150 ns and a total amplitude of positive and negative components of ± 20 -60 kV. The generator of high-voltage nanosecond pulses is built according to the scheme with resonant recharging of the storage low-inductance capacitor with a capacity of 1540 pF. The TGI-1000-25 hydrogen pulse thiratron served as the commutator in the modulator. The frequency of repetition of voltage pulses could vary between 40-1000 Hz.

An overvoltage nanosecond discharge was ignited at a distance between the electrodes of 2 mm between their end parts with a radius of 10 mm. The diameter of the electrodes was 5 mm.

Oscillograms of voltage pulses on the discharge gap and oscillograms of current pulses were recorded using a broadband capacitive voltage divider, a Rohovsky coil and a broadband oscilloscope 6LOR-04. The time separation of this system for measuring the characteristics of electric pulses was 2-3 ns.

A digital two-channel spectrometer with astigmatism compensation "SL-40-2-1024USB" was used to record plasma radiation spectra. Working range of the spectrometer: 200-1200 nm. The absolute radiation power of the point lamp was measured using the ultraviolet absolute radiation power meter "TKA-PKM".

A nanosecond discharge was ignited by overvoltage of the discharge gap, when a beam of runaway electrons is formed in it [7]. Under the action of this beam and accompanying X-ray radiation, the discharge in argon was uniform even with a rather heterogeneous distribution of the electric field strength between electrodes with radii of rounding of hemispherical working surfaces (~ 10 mm). The discharge aperture was close to square and was about 4 mm². In a strong electric field on the working surface of the electrode based on the superionic conductor Ag₂S, microexplosions of nanowisters occur on the surface of the electrodes, which contributed to the introduction of vapors of the superionic conductor Ag₂S products and their decay (Ag, Ag⁺, S ...) into the plasma and their deposition on a glass substrate in the form of a thin film based on the Ag₂S compound. The presence of Ag₂S molecules in the discharge gap at the initial moments of time from the breakdown, which can be considered as an impurity that is easily ionized, also contributes to obtaining a uniform discharge [5].

When the glass substrate was installed at a distance of 2-4 cm from the center of the discharge gap and the burning time of the discharge was 30-60 minutes, the deposition of a thin film from the products of sputtering of the electrode material was recorded on the substrate. The obtained samples of thin films were studied using the "XploRA PLUS" Raman spectrometer, which also made it possible to obtain images of the film surface.

When conducting experimental research, a digital two-channel spectrometer with astigmatism compensation "SL-40-2-1024USB" and a Raman scattering (Raman) spectrometer "XploRA PLUS" of the Center for the Collective Use of Scientific Equipment "Laboratory of Experimental and Applied Physics" at the Uzhhorod National University" were used.

Characteristics of the Discharge

In Fig. 1. the oscillograms of current and voltage pulses, the pulsed power of an overvoltage nanosecond discharge between the electrodes from the Ag₂S compound in atmospheric pressure argon and the energy contribution to the plasma for one pulse are given.

In this experiment, the total duration of voltage pulses reached 400-450 ns, and the voltage pulse itself consisted of time-decaying oscillations with a duration of about 40-50 ns. Within these oscillations, short-duration oscillations of 5-10 ns also appeared. The maximum voltage drop of one polarity on the discharge gap was 22 kV. The maximum amplitude of the current pulse of one polarity reached 100 A. The highest value of the impulse power of the discharge was reached in the first 120 ns from the moment of its ignition and was about 3 MW (at $t = 110$ -120 ns). The second and third pulse power maxima were about 1 MW and were observed at the time from the start of discharge ignition $t = 175$ -300 ns. The energy of a single electric pulse was about 119 ± 12 mJ.

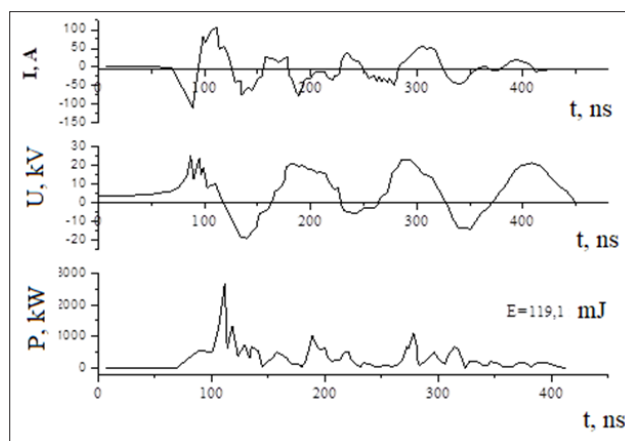


Figure 1: Oscillograms of current pulses, voltages, pulse power and energy contribution to an overvoltage nanosecond discharge for one pulse ($p(\text{Ar}) = 101$ kPa, $f = 1000$ Hz, $d = 2$ mm).

An increase in the voltage on the anode of the thiratron from 12 to 20 kV and a small fixed frequency of repetition of pulses at the level of 80 Hz led to a twofold increase in the intensity of UV radiation.

Increasing the frequency from 350 to 1000 Hz led to an increase in the intensity of UV radiation in all ranges by 5-10 times. At the same time, the maximum increase in the intensity of UV radiation was in the spectral range $\Delta\lambda = 315$ -400 nm.

Table 1: shows the UV radiation power of the discharge at different argon pressures.

The total power of the UV radiation of the discharge on the surface of the solid substrate, where the thin films were synthesized and which was placed at a distance of 2-3 cm from the electrode system, was 0.5-0.8 W.

Table 1: Maximum values of UV power - discharge radiation at different argon pressures (U=20 kV, f=1000 Hz, d=2 mm).

Spectral range	p(argon)= 13.3 kPa	p(argon)= 50.5 kPa	p(argon)= 101 kPa
	W, a.u..	W, a.u..	W, a.u..
УФ-C (200-280ns)	8.8	16.3	26
УФ-B (280 - 315 ns)	5.5	7	9
УФ-A (315-400 ns)	13.9	32	48

When studying the spectral characteristics of a discharge between electrodes made of silver sulfide, a control experiment was conducted to study the radiation spectra of this discharge, but between electrodes made of pure silver. Such an experiment made it possible to obtain information about the degree of dissociation of silver sulfide molecules and the release of silver atoms from the Ag₂S compound in the discharge between the electrodes.

Ultraviolet radiation spectra of plasma based on silver and silver sulfide at atmospheric pressure of argon and a distance between electrodes of 2 mm are shown in Figure 4 and 5., and the results of the identification of spectral lines in these spectra are shown in Tables 2 and 3. The reference was used to identify the spectral lines of the discharge plasma radiation spectrum[8].

As can be seen from Figure 4 and 5 and Tables 2 and 3, the ultraviolet spectra of plasma radiation of pure silver and silver sulfide compounds are almost identical to the radiation objects of atoms and singly charged silver ions, but differ in the distribution of the radiation intensity of these spectral lines of atoms and singly

charged silver ions. This may be due to the peak structure of voltage pulses (Figure 2). The peak structure on the current pulses is absent due to the low resolution of the current sensor, which did not exceed 20 ns. The very first peaks of voltage (current) lead to the dissociation of silver sulfide molecules, as a result of which mainly silver atoms remain in the discharge gap (as in the case of discharge between silver electrodes). Therefore, when modeling the discharge plasma parameters in silver sulfide vapors using the Boltzmann equation for the electron energy distribution function (EEDF), it is possible to use a set of effective cross sections of electronic processes (elastic scattering of electrons, excitation, and ionization) for a silver atom. Currently, such effective sections of electronic processes have not been established. Cross sections of electronic processes are unknown for silver sulfide molecules, but for silver atoms they are known and we used them in the calculations.

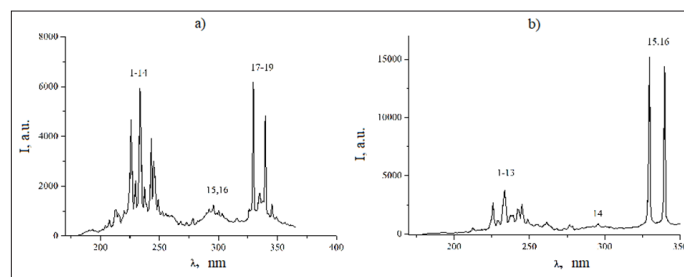


Figure 4: UV - spectrum of plasma radiation of an overvoltage nanosecond discharge between silver electrodes at atmospheric air pressure (a) and between Ag₂S compound electrodes (b) at p(Ar) = 101 kPa; f=1000 Hz, d=2mm.

Table 2: The results of identification of the radiation spectra of the discharge plasma between silver electrodes at atmospheric air pressure and between silver sulfide electrodes at p(Ar) = 101 kPa and d = 2 mm; f=1000 Hz.

№	λ _{tab} , nm	I _{exp} , a. u. electrodes from silver	I _{exp} , a. u. electrodes from silver sulfide	Object	E _{low} , eV	E _{up} , eV	Lower _{term}	Upper _{term}
1	206.59	646	340	Ag II	5.05	11.05	4d ⁹ (² D _{3/2})5s 2[⁵ / ₂] ₂	4d ⁹ (² D _{3/2})5p 2[⁵ / ₂] ₃
2	211.38	1056	-	Ag II	4.85	10.71	4d ⁹ (² D _{3/2})5s 2[⁵ / ₂] ₃	4d ⁹ (² D _{3/2})5p 2[⁵ / ₂] ₃
3	214.56	892	-	Ag II	5.42	11.20	4d ⁹ (² D _{3/2})5s 2[³ / ₂] ₁	4d ⁹ (² D _{3/2})5p 2[¹ / ₂] ₁
4	218.67	1020	-	Ag II	5.05	10.71	4d ⁹ (² D _{3/2})5s 2[⁵ / ₂] ₂	4d ⁹ (² D _{3/2})5p 2[⁵ / ₂] ₃
5	224.64	4661	1363	Ag II	4.85	10.37	4d ⁹ (² D _{3/2})5s 2[⁵ / ₂] ₃	4d ⁹ (² D _{3/2})5p 2[⁷ / ₂] ₄
6	227.99	2219	992	Ag II	5.70	11.14	4d ⁹ (² D _{3/2})5s 2[³ / ₂] ₂	4d ⁹ (² D _{3/2})5p 2[³ / ₂] ₁
7	232.02	5932	1418	Ag II	5.70	11.05	4d ⁹ (² D _{3/2})5s 2[³ / ₂] ₂	4d ⁹ (² D _{3/2})5p 2[⁵ / ₂] ₃
8	233.13	3853	2473	Ag II	5.05	10.36	4d ⁹ (² D _{3/2})5s 2[⁵ / ₂] ₂	4d ⁹ (² D _{3/2})5p 2[³ / ₂] ₁
9	241.13	1951	1005	Ag II	5.42	10.56	4d ⁹ (² D _{3/2})5s 2[³ / ₂] ₁	4d ⁹ (² D _{3/2})5p 2[⁵ / ₂] ₂
10	243.77	3926	1901	Ag II	4.85	9.94	4d ⁹ (² D _{3/2})5s 2[⁵ / ₂] ₃	4d ⁹ (² D _{3/2})5p 2[³ / ₂] ₂
11	244.78	2990	1413	Ag II	5.70	10.77	4d ⁹ (² D _{3/2})5s 2[³ / ₂] ₂	4d ⁹ (² D _{3/2})5p 2[⁵ / ₂] ₂
12	260.59	825	553	Ag II	10.18	14.94	4d ⁹ (² D _{3/2})5p 2[⁷ / ₂] ₃	4d ⁹ (² D _{3/2})6s 2[⁵ / ₂] ₃

13	261.43	768	644	Ag II	10.77	15.51	$4d^9(^2D_{3/2})5p$ $2[5/2]_2^{\circ}$	$4d^9(^2D_{3/2})6s$ $2[3/2]_1$
14	266.04		245	Ag II	12.14	16.78	$4d^85s^2\ ^3F_3$	$4d^8(^3F)5s5p(^3P^{\circ})$ $^5G_2^{\circ}$
15	271.18	543	276	Ag II	10.37	14.94	$4d^9(^2D_{5/2})5p$ $2[7/2]_4^{\circ}$	$4d^9(^2D_{5/2})6s$ $2[5/2]_3$
16	276.75	711	480	Ag II	5.70	10.18	$4d^9(^2D_{3/2})5s$ $2[3/2]_2$	$4d^9(^2D_{3/2})5p$ $2[7/2]_3^{\circ}$
17	293.83	1232	619	Ag II	10.77	14.99	$4d^9(^2D_{3/2})5p$ $2[5/2]_2^{\circ}$	$4d^9(^2D_{3/2})6s$ $2[5/2]_2$
18	328.06	6187	14166	Ag I	0.00	3.77	$4d_{10}5s\ ^2S_{1/2}$	$4d^{10}5p\ ^2P_{3/2}^{\circ}$
19	333.13	1736	-	N II	20.65	24.37	$2s^22p3p$ 3D_2	$2s^22p4s$ $^3P_1^{\circ}$
20	338.28	4820	12136	Ag I	0.00	3.66	$4d^{10}5s$ $^2S_{1/2}$	$4d^{10}5p$ $^2P_{1/2}^{\circ}$

The investigated plasma emits mainly in the spectral range of 200-340 nm. The main sources of radiation in the short-wave spectral range of 200-300 nm were singly charged silver ions, and in the spectral range of 300-340 nm - silver atoms. The most intense spectral lines in the spectral range of 200-400 nm were the spectral lines of the silver atom, for which the lower energy level is the ground state of the silver atom (lines 15 and 16 of Table 3).

When reducing the frequency to 80 Hz and the argon pressure to 13.3 kPa, a significant decrease in the intensity of the spectral lines of silver was observed (Figure 3), which is caused by a decrease in the concentration of the electrode material and its decomposition products in the plasma.

Table 3 Shows The Results of Identification of This Radiation Spectrum.

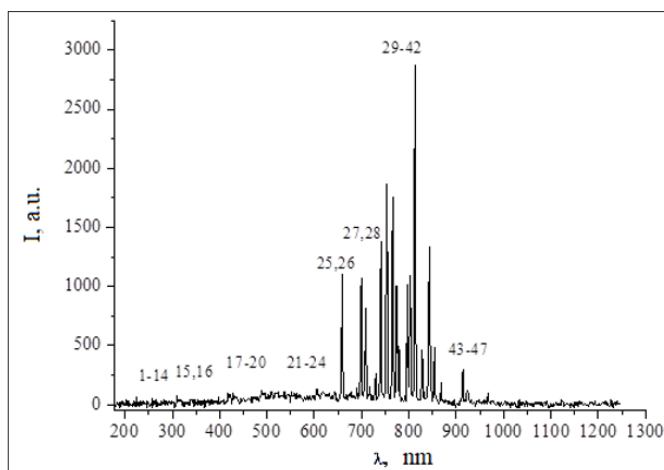


Figure 3: The radiation spectrum of a high-voltage nanosecond discharge between Ag₂S electrodes at an argon pressure of 13.3 kPa (f=80 Hz).

Table 3: Results of identification of plasma radiation spectra of a discharge between Ag₂S electrodes at an argon pressure of 13.3 kPa (d=2 mm; f=80 Hz).

№	λ tab, nm	I exp a. u.	Object	Elow., eV	Eup., eV	Lower term	Upper term
1	211.38	9	Ag II	4.85	10.71	$4d^9(^2D_{5/2})5s$ $2[5/2]_3$	$4d^9(^2D_{5/2})5p$ $2[5/2]_3^{\circ}$
2	224.64	65	Ag II	4.85	10.37	$4d^9(^2D_{5/2})5s$ $2[5/2]_3$	$4d^9(^2D_{5/2})$ $5p\ 2[7/2]_4^{\circ}$
3	227.99	24	Ag II	5.70	11.05	$4d^9(^2D_{3/2})5s$ $2[3/2]_2$	$4d^9(^2D_{3/2})5p$ $2[5/2]_3^{\circ}$
4	232.02	15	Ag II	5.05	10.36	$4d^9(^2D_{5/2})5s$ $2[5/2]_2$	$4d^9(^2D_{5/2})5p$ $2[3/2]_1^{\circ}$
5	233.13	15	Ag II	5.05	10.36	$4d^9(^2D_{5/2})5s$ $2[5/2]_2$	$4d^9(^2D_{5/2})5p$ $2[3/2]_1^{\circ}$

6	241.13	13	Ag II	5.42	10.56	$4d^9(^2D_{3/2})5s$ $2^3[2]_1$	$4d^9(^2D_{5/2})5p$ $2^5[2]_2$
7	243.77	8	Ag II	4.85	9.94	$4d^9(^2D_{5/2})5s$ $2^5[2]_3$	$4d^9(^2D_{5/2})$ $5p 2^3[2]_2^6$
8	244.78	11	Ag II	5.70	10.77	$4d^9(^2D_{3/2})5s$ $2^3[2]_2$	$4d^9(^2D_{3/2})5p$ $2^5[2]_2$
9	260.59	10	Ag II	10.18	14.94	$4d^9(^2D_{5/2}) 5p$ $2^7[2]_3$	$4d^9(^2D_{5/2})6s$ $2^5[2]_3$
10	261.43	29	Ag II	10.77	15.51	$4d^9(^2D_{3/2})5p$ $2^5[2]_2$	$4d^9(^2D_{3/2})6s$ $2^3[2]_1$
11	266.04	2	Ag II	12.14	16.78	$4d^85s^2 \ ^3F_3$	$4d^8(^3F)5s5p(^3P^o)$ $^5G^o_2$
12	271.17	4	Ag II	10.37	14.94	$4d^9(^2D_{5/2}) 5p$ $2^7[2]_4$	$4d^9(^2D_{5/2}) 6s$ $2^5[2]_3$
13	276.75	27	Ag II	5.70	10.18	$4d^9(^2D_{3/2})5s$ $2^3[2]_2$	$4d^9(^2D_{5/2})5p$ $2^7[2]_3$
14	293.83	32	Ag II	10.77	14.99	$4d^9(^2D_{3/2})5p$ $2^5[2]_2$	$4d^9(^2D_{5/2})6s$ $2^5[2]_2$
15	328.06	5	Ag I	0.00	3.77	$4d^{10}5s \ ^2S_{1/2}$	$4d^{10}5p \ ^2P^o_{3/2}$
16	338.28	41	Ag I	0.00	3.66	$4d^{10}5s$ $^2S_{1/2}$	$4d^{10}5p$ $^2P^o_{1/2}$
17	405.54	30	Ag I	3.66	6.72	$4d^{10}5p$ $2P^o \ ^1_2$	$4d^{10}6d$ $^2D_{3/2}$
18	424.06	70	Ag II	14.08	17.00	$4d^85s^2 \ ^1G_4$	$4d^9(^2D_{3/2})6p$ $2^5[2]_3$
19	425.93	50	Ar I	11.82	14.73	$3s^23p^5(^2P^o_{1/2})$ $4s 2^1[2]_0^1$	$3s^23p^5(^2P^o_{1/2})5p$ $2^1[2]_0$
20	433.11	57	Ar I	16.74	19.61	$3s^23p^4(^3P) 4s$ $^4P_{3/2}$	$3s^23p^4(^3P)4p$ $^4D^o_{3/2}$
21	490.24	101	S II	15.55	18.08	$3s^23p^2(^3P)4p$ $^2S^o_{1/2}$	$3s3p^4$ $^2P_{1/2}$
22	520.90	105	Ag I	3.66	6.04	$4d^{10}5p \ ^2P^o_{1/2}$	$4d^{10}5d \ ^2D_{3/2}$
23	531.24	79	Ag II	15.70	18.03	$4d^9(^2D_{5/2})5d$ $2^9[2]_4$	$4d^9(^2D_{5/2}) 4f$ $2^9[2]_4$
24	547.86	88	Ag II	15.71	17.97	$4d^9(^2D_{5/2})5d$ $2^3[2]_2$	$4d^9(^2D_{5/2})4f$ $2^1[2]_1$
25	657.07 - second order 328.06	1106	Ag I	0.00	3.77	$4d^{10}5s \ 2S_{1/2}$	$4d^{10}5p \ ^2P^o_{3/2}$
26	679.2 - second order 338.28	63	Ag I	0.00	3.66	$4d^{10}5s$ $^2S_{1/2}$	$4d^{10}5p$ $^2P^o_{1/2}$
27	696.54	1074	Ar I	11.54	13.32	$3s^23p^5(^2P^o_{3/2})$ $4s 2^3[2]_2$	$3s^23p^5(^2P^o_{1/2})4p$ $2^1[2]_1$
28	706.72	813	Ar I	11.54	13.30	$3s^23p^5(^2P^o_{3/2})$ $4s 2^3[2]_2$	$3s^23p^5(^2P^o_{1/2})4p$ $2^3[2]_2$
29	727.29	270	Ar I	11.62	13.32	$3s^23p^5(^2P^o_{3/2})$ $4s 2^3[2]_1$	$3s^23p^5(^2P^o_{1/2})4p$ $2^1[2]_1$
30	731.60	61	Ar I	13.32	15.02	$3s^23p^5(^2P^o_{1/2})4p$ $2^1[2]_1$	$3s^23p^5(^2P^o_{1/2})6s^2$ $[1/2]_1$
31	738.39	1383	Ar I	11.62	13.30	$3s^23p^5(^2P^o_{3/2})4s$ $2^3[2]_1$	$3s^23p^5(^2P^o_{1/2})4p$ $2^3[2]_2$
32	751.46	1870	Ar I	11.62	13.27	$3s^23p^5(^2P^o_{3/2})4s$ $2^3[2]_1$	$3s^23p^5(^2P^o_{3/2})4p$ $2^1[2]_0$
33	763.51	1751	Ar I	11.54	13.17	$3s^23p^5(^2P^o_{3/2})4s$ $2^3[2]_2$	$3s^23p^5(^2P^o_{3/2})4p$ $2^3[2]_2$

34	772.42	1005	Ar I	11.72	13.32	$3s^23p^5(^2P^{\circ}_{1/2})4s\ 2[1/2]^{\circ}0$	$3s^23p^5(^2P^{\circ}_{1/2})4p\ 2[1/2]_1$
35	794.81	1011	Ar I	11.72	13.28	$3s^23p^5(^2P^{\circ}_{1/2})4s\ 2[1/2]^{\circ}0$	$3s^23p^5(^2P^{\circ}_{1/2})4p\ 2[3/2]_1$
36	800.51	153	Ag II	14.94	16.49	$4d^9(^2D_{5/2})6s\ 2[5/2]_3$	$4d^9(^2D_{5/2})6p\ 2[5/2]_3$
37	801.46	1094	Ar I	11.54	13.09	$3s^23p^5(^2P^{\circ}_{3/2})4s\ 2[3/2]^{\circ}2$	$3s^23p^5(^2P^{\circ}_{3/2})4p\ 2[5/2]_2$
38	811.53	2873	Ar I	11.54	13.07	$3s^23p^5(^2P^{\circ}_{3/2})4s\ 2[3/2]^{\circ}2$	$3s^23p^5(^2P^{\circ}_{3/2})4p\ 2[5/2]_3$
39	826.45	462	Ar I	11.82	13.32	$3s^23p^5(^2P^{\circ}_{1/2})4s\ 2[1/2]^{\circ}1$	$3s^23p^5(^2P^{\circ}_{1/2})4p\ 2[1/2]_1$
40	842.46	1335	Ar I	11.62	13.09	$3s^23p^5(^2P^{\circ}_{3/2})4s\ 2[3/2]^{\circ}1$	$3s^23p^5(^2P^{\circ}_{3/2})4p\ 2[5/2]_2$
41	852.14	483	Ar I	11.82	13.28	$3s^23p^5(^2P^{\circ}_{1/2})4s\ 2[1/2]^{\circ}1$	$3s^23p^5(^2P^{\circ}_{1/2})4p\ 2[3/2]_1$
42	869.47	188	S I	7.86	9.29	$3s^23p^3(^4S^{\circ})4p\ 5P_3$	$3s^23p^3(^4S^{\circ})4d\ 5D^{\circ}_4$
43	912.3	296	Ar I	11.54	12.90	$3s^23p^5(^2P^{\circ}_{3/2})4s\ 2[3/2]^{\circ}2$	$3s^23p^5(^2P^{\circ}_{3/2})4p\ 2[1/2]_1$
44	922.44	120	Ar I	11.82	13.17	$3s^23p^5(^2P^{\circ}_{1/2})4s\ 2[1/2]^{\circ}1$	$3s^23p^5(^2P^{\circ}_{3/2})4p\ 2[3/2]_2$
45	942.19	34	S I	8.40	9.72	$3s^23p^3(^2D^{\circ})4s\ 3D^{\circ}_2$	$3s^23p^3(^2D^{\circ})4p\ 3F_3$
46	964.95	25	S I	8.41	9.69	$3s^23p^3(^2D^{\circ})4s\ 3D^{\circ}_3$	$3s^23p^3(^2D^{\circ})4p\ 3D_3$
47	965.77	103	Ar I	11.62	12.90	$3s^23p^5(^2P^{\circ}_{3/2})4s\ 2[3/2]^{\circ}1$	$3s^23p^5(^2P^{\circ}_{3/2})4p\ 2[1/2]_1$

At the same time, visible and infrared radiation of argon and sulfur atoms becomes the main spectrum.

Therefore, the spectral characteristics of the discharge between silver sulfide electrodes showed that for the synthesis of thin films from the material of the electrodes, the optimal operating mode of the reactor was achieved at an atmospheric pressure of argon of 101 kPa and a pulse repetition frequency of 1000 Hz.

Figure 4: shows characteristic oscillograms of the emission of spectral lines of silver in a discharge between electrodes with Ag₂S at an argon pressure of 101 kPa.

The maximum radiation intensity is 89 arb. unit was obtained for the spectral line 293.83 nm of Ag II; it was reached at time $t = 80$ ns.

Maximum radiation intensity – 52.52 arb. unit for the spectral line of 424.06 nm Ag II was reached at $t = 126$ ns.

The maximum radiation intensity is 63 relative units. for the spectral line of 328.06 nm Ag I was reached at $t = 103$ ns.

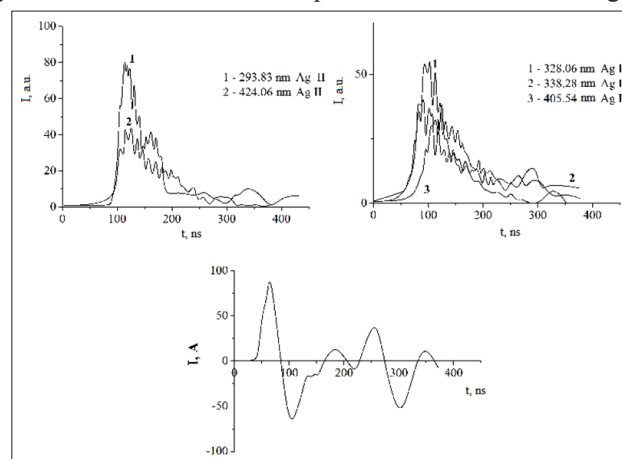


Figure 4: Oscillograms of radiation of spectral lines of an atom and a singly charged silver ion and an oscillogram of the current of an overvoltage nanosecond discharge between electrodes with Ag₂S at an argon pressure of 101 kPa.

The maximum radiation intensity is 45 arb. units. for the 338.28 nm spectral line of Ag I was reached at $t = 92$ ns.

The maximum radiation intensity is at the level of 47 arb. units for the 405.54 nm spectral line of Ag II was reached at $t = 125$ ns.

The maximum current of 92 A was reached at time $t = 62$ ns.

All the oscillograms of the spectral lines of the silver atom and ion had a peak radiation structure caused by the peak shape of the voltage on the discharge gap (the duration of individual peaks is 5-10 ns). The total maximum of the radiation intensity of the silver lines was in the afterglow of the main current maximum ($t = 62$ ns). This may be due to the recombination nature of the radiation of silver atoms and ions in this experiment.

When installing a solid substrate made of dielectric at a distance of 2-3 cm from the center of the interelectrode gap and with a burning time of 30-60 minutes on the substrate, the deposition of microstructures from the products of sputtering of the electrode material in atmospheric pressure argon was recorded (Figure 5). The characteristic sizes of surface microstructures are 10-20 μm .

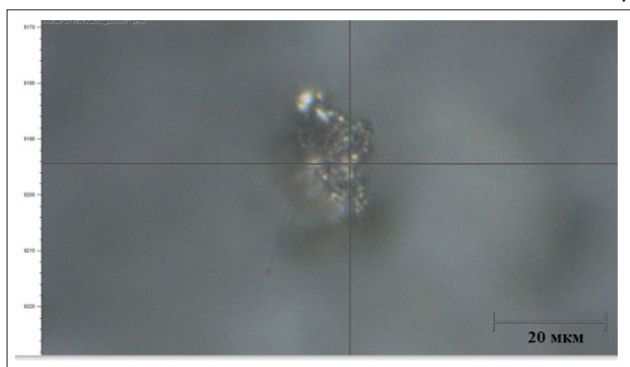


Figure 5: Photo of the surface microstructure, which was deposited from the plasma of a high-voltage nanosecond discharge between the electrodes of the polycrystalline compound Ag_2S in argon.

The study of the spectra of light scattering by the synthesized structures by the method of micro-Raman spectroscopy under the conditions described in showed that they consist only of silver sulfide [8].

Plasma Parameters

The parameters of the discharge plasma in the gas-vapor mixture “argon - silver” at an argon pressure of 101000-500 Pa were calculated numerically as total integrals of the energy distribution function of electrons in the discharge. The FREE was found by solving the Boltzmann kinetic equation in the binomial approximation using the program [9]. Average electron energies, electron temperatures, electron drift velocities, electron concentrations, excitation rate constants of energy levels of silver atoms, as well as specific discharge losses due to elastic and inelastic processes of collisions of electrons with atoms of both mixtures depending on the magnitude of the reduced electric field were determined on the basis of the calculated EEDF(E) to the total concentration of argon atoms and silver atoms (N).

Plasma parameters were determined from ratios [10-12].

The range of changes of the parameter $E/N=1-1000$ Td ($1 \cdot 10^{-17} - 1 \cdot 10^{-14} \text{ V} \cdot \text{cm}^2$) and included the values of the reduced electric field that were implemented in the experiment. These values of the reduced electric field were 406 Td and 346 Td for the time of 70 ns and 130 ns voltage pulses (Figure 2) from the start of the

discharge. The following processes are taken into account in the integral of collisions of electrons with atoms: elastic scattering of electrons on silver atoms, excitation of energy levels of atoms and silver ions (threshold energies of 6.01 eV, 3.78 eV, 3.66 eV, 7.19 eV, 7.02 eV, 6.71 eV, 5.99 eV and 17 eV), ionization of silver atoms (threshold energy 8.00 eV); elastic scattering of electrons on argon atoms, excitation of the energy level of argon atoms (threshold energy 11.50 eV), ionization of argon atoms (threshold energy 15.80 eV).

Data on the absolute values of the effective cross sections of these processes, as well as their dependence on electron energies, are taken from the database of articles [13-14].

The mean energy of the discharge electrons for vapor-gas mixtures of silver-argon sulfide increases almost linearly from 1.349 eV to 4.214 eV with an increase in the reduced electric field strength from 1 Td to 35 Td. At the same time, a pattern of increased rate of change was observed in this range of reduced electric field strength compared to the range of 35-1000 Td. For the range of reduced electric field strength 406 Td - 346 Td, in which experimental studies of electrical and optical characteristics of the discharge were carried out, the mean energies of electrons varied within 9.323-8.722 eV (Fig. 8). Their highest energies corresponded to values of 121.2 eV - 103.9 eV.

Table 4 shows the results of calculating electron transport characteristics: mean energy (ϵ), temperature (T^0 K), drift velocity (V_{dr}) and electron concentration (N_e) for a mixture of silver sulfide vapors with argon.

Table 4: Transport characteristics of electrons for the mixture: $\text{Ag}_2\text{S}-\text{Ar}=500$ Pa - 101300 Pa

τ , ns	E/N, Td	Mixtures: $\text{Ag}_2\text{S}-\text{Ar}=500$ Pa - 101300 Pa			
		ϵ , eV	T^0 , K	V_{dr} , m/s	N_e , m^{-3}
70	406	9.323	108 147	$2.7 \cdot 10^5$	$1.18 \cdot 10^{20}$
130	346	8.722	101 175	$2.1 \cdot 10^5$	$1.12 \cdot 10^{20}$

The temperature and electron drift velocities (table 4) decreases from 108 147 K to 101 175 K and from $2.7 \cdot 10^5$ m/c to $2.1 \cdot 10^5$ m/c when the reduced electric field strength changes from 406 Td to 346 Td, respectively. The electron concentration values decrease from $1.18 \cdot 10^{20} \text{m}^{-3}$ to $1.12 \cdot 10^{20} \text{m}^{-3}$.

Conclusions

A study of the characteristics and parameters of a plasma of a high-voltage nanosecond discharge in atmospheric pressure argon between electrodes made of the Ag_2S compound revealed the following at a distance between the electrodes of ~ 2 mm, a homogeneous discharge was ignited, the shape of which was determined by the energy contribution to the plasma and the pulse repetition frequency. The maximum voltage of one polarity on the discharge gap reached 22 kV with its full duration up to 450 ns, and individual oscillations on the voltage pulse had a duration of 5-10 ns; the maximum amplitude of the current pulses was 100 A, the value of the pulse electric power reached 10 MW with the energy in a single pulse - 119 mJ. The maximum intensity of discharge radiation on the surface of a solid substrate, on which thin films of electrode material were deposited, in the spectral range of 200-400 nm reached 0.5-0.8 W. The spectrum of the ultraviolet radiation of the discharge was dominated by the radiation of atoms of singly charged silver ions in the spectral range of 200-300 nm and of silver atoms in the spectral range of 300-340 nm, which is

promising for the development of a spot UV lamp based on the vapors of the Ag_2S compound for applications in nanotechnology, medicine and biology. The maximum intensity of UV radiation of silver atoms and ions was obtained at $p(\text{Ar}) = 101 \text{ kPa}$ and $f = 1000 \text{ Hz}$. Numerical modeling of plasma parameters of the studied discharge showed that for the range of reduced electric field strength 346 - 406 Td, in which the experiment was conducted, the mean electron energy was in the range of 9.32 - 8.72 eV. The value of the electron concentration reached $1.18 \cdot 10^{20} \text{ m}^{-3}$.

References

1. Shuaibov OK, Malinina AO (2021) Overstressed Nanosecond Discharge in the Gases at Atmospheric Pressure and Its Application for the Synthesis of Nanostructures Based on Transition Metals. *Progress in Physics of Metals* 22: 382-439.
2. Shuaibov OK, Hrytsak RV, Minya OI, Malinina AA, Bilak Yu Yu, et al. (2022) Spectroscopic diagnostic of overstressed nanosecond discharge plasma between zinc electrodes in air and nitrogen. *Journal of Physical Studies* 26: 1-8.
3. Mesyats GA (1995) Ecton-Electron Avalanche from metal. *Usp. Fizich. Nauk.* 165: 601-626.
4. Tominaga, N Umezu, I Mori, T Ushiro, T Moriga, et al. (1998) Effects of UV light irradiation and excess Zn addition on ZnO: Al film properties in sputtering process. *Thin Solid Films* 316: 85-88.
5. Tolstoguzova AB, Belykh SF, Gololobova GP, Gurova VS, Guseva SI, et al. (2018) Ion sources on solid electrolytes for aerospace applications and ion-beam technologies (review) // *Instruments and Experimental Technology* 2: 5-19.
6. Shuaibov OK, Mynia OY, Malinin OM, Hrytsak RV, Malinina AO, (2023) *Journal of Nano-and Electronic Physics* https://jnep.sumdu.edu.ua/en/full_article/3636.
7. Tarasenko VF, Evgenii H Baksht, Alexander G Burachenko, Igor D Kostyrya, Mikhail I Lomae (2014) *Runaway electrons preionized diffuse discharge*. New York: Nova Science Publishers Inc. <https://ieeexplore.ieee.org/document/5227677/authors>.
8. NIST Atomic Spectra Database Lines Form [https:// physics.nist.gov/ PhysRefData/ASD/lines_form.html](https://physics.nist.gov/PhysRefData/ASD/lines_form.html).
9. <http://www.bolsig.laplace.univ-tlse.fr>.
10. Frost LS, Phelps AV (1982) Rotation excitation and momentum transfer cross sections for electrons in H and N from transport coefficients. *Phys Rev* 127: 1621-1633.
11. Shlie LA (1976) Electron velocity distributions fractional energy transfer and collisional raser for potential Na, NaHe and NaXe electrically excited laser discharge. *J Appl Phys* 47: 1307-1407.
12. Smirnov Yu M (1999) Cross section of excitation of a silver atom by electron impact, *Journal of Technical Physics* 69: 6-10.
13. Dhanoj Gupta, Rahla Nagma, Bobby Antony (2013) Electron impact total and ionization cross sections for Sr, Y, Ru, Pd, and Ag atoms Electron impact total and ionization cross sections for Sr, Y, Ru, Pd, and Ag atoms, *Can. J Phys* 91: 744-750.
14. Yu M Smirnov (1999) Excitation of Cu II and Ag II in electron-atom collisions. *Quantum Electronics* 29: 168-172.

Copyright: ©2023 OK Shuaibov, et al. This is an open-access article distributed under the terms of the Creative Commons Attribution License, which permits unrestricted use, distribution, and reproduction in any medium, provided the original author and source are credited.